# Fungal Metabolites. Part 7.† Solution Structure of an Antibiotic Peptide, Trichosporin B-V, from *Trichoderma polysporum*

**Akira Iida,[a] Shinichi Uesato,[a] Tetsuro Shingu,[b] Yasuo Nagaoka,[a] Yoshihiro Kuroda[a] and Tetsuro Fujita*[a]**
[a] *Faculty of Pharmaceutical Sciences, Kyoto University, Sakyo-ku, Kyoto 606, Japan*
[b] *Faculty of Pharmaceutical Sciences, Kobe Gakuin University, Kobe 658, Japan*

The secondary structure of the peptaibol trichosporin B-V in methanol was investigated in detail by 600 MHz nuclear magnetic resonance spectroscopy. Its fundamental secondary structure was characterized as a helix by the circular dichroism spectrum. Inter-residual nuclear Overhauser effect patterns, $^3J_{NH\text{-}C\alpha H}$ amide coupling constants, hydrogen–deuterium (H–D) exchange rates of the amide protons, and inspection of molecular models showed that the secondary structure of this peptide consists of two major α-helical structures because of a bent structure around a Pro residue, and that the first three amino acid residues of the *N*-terminal α-helix are arranged predominantly in a $3_{10}$-helical fashion.

Trichosporin (TS)-Bs,[1,2] isolated from the culture broth of the fungus *Trichoderma polysporum*, are linear eicosapeptides belonging to the class of peptaibols such as alamethicin[3] and suzukacillin.[4] In the preceding paper,[5] we have already described how the conformations of TS-Bs are very similar to each other in methanol, but we did not refer to the fine detail of secondary structures; basically, TS-Bs adopt helical conformations (Fig. 1), as do other peptaibols[4,6,7] and their analogues owing to α-aminoisobutyric acid (Aib) residues stabilizing α-helices.[8]

In this paper, we discuss the secondary structure of the main component, TS-B-V, through analyses of its NMR spectra recorded in methanol.

Trichosporin-B-V: Ac-Aib-Ala-Ala-Ala-Aib-Aib-Gln-Aib-Ile-Aib-Gly-Leu-Aib-Pro-Val-Aib-Aib-Gln-Gln-Pheol (Pheol = phenylalaninol).

## Results and Discussion

*$^3J_{NH-C\alpha H}$ Amide Coupling Constants.*— Amide coupling constants. ($^3J_{NH-C\alpha H}$) reflect peptide conformations in solution.[9] The values at −5, 10, 25 and 40 °C are listed in Table 1. Regardless of temperature, most values are less than 7 Hz. These small values strongly suggest that the *N*-terminal fragment between Ac-Aib and Gly[11] preferentially adopts a helical structure. On the other hand, the values of Leu[12], Val[15], Gln[19] and Pheol[20] are higher, which suggests the presence of a β-pleated sheet with intermolecular hydrogen bonding.[10] However, we have already demonstrated that TS-B-V does not aggregate by intermolecular hydrogen bonding in methanol.[5] Therefore this structure can be ruled out. As shown Fig. 1, the CD absorptions at 207 and 221 nm of des-Pro[14]-TS-B-V increased compared with TS-B-V; compound des-Pro[14]-TS-B-V was synthesized according the procedure reported previously.[11] This observation indicates that the helical content of the analogue is higher than that of the natural peptide. In addition, the Leu[12] and Val[15] $^3J_{NH-C\alpha H}$-values of the analogue are small in comparison with those of TS-B-V (Table 2). This shows that the Leu[12] and Val[15] residues of the analogue are arranged in a regular helical fashion. Thus, it is clear that the *J*-values of Leu[12] and Val[15] are suggestive of a conformational deviation caused by the presence of a Pro residue.

The $^3J_{NH-C\alpha H}$-values were almost temperature independent over the range of 10–40 °C. This result indicates that the backbone conformation of this peptide hardly changes up to

† Part 6, ref. 5.

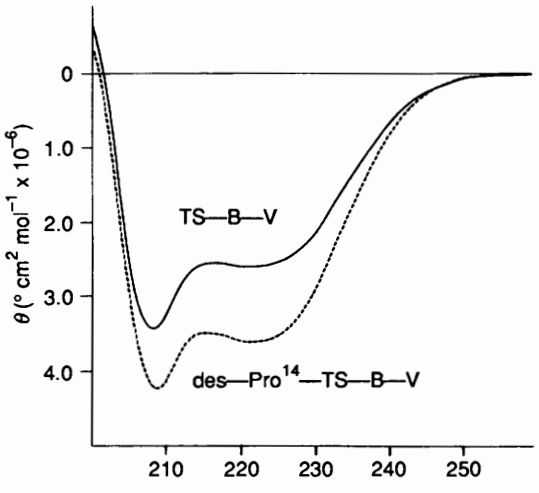


**Fig. 1** CD spectra of trichosporin B-V and des-Pro[14]-trichosporin B-V in MeOH (25 °C). Both spectra show, typically, two negative Cotton effects, at 207 and 221 nm, for a right-handed helical conformation. Molecular ellipticity, θ (° cm² mol⁻¹), at 221 and 207 nm: −2.589 × 10⁵ and −3.305 × 10⁵ (TS-B-V), −3.601 × 10⁵ and −3.936 × 10⁵ (des-Pro[14]-TS-B-V).

**Table 1** Temperature dependence of the $^3J_{NH-C\alpha H}$-values of trichosporin B-V in $CD_3OH$ at 10 mmol dm$^{-3}$

| Residue | −5 °C *J*/Hz | 10 °C *J*/Hz | 25 °C[a] *J*/Hz | 40 °C[b] *J*/Hz |
|---|---|---|---|---|
| Ala[2] | 3.5 | 3.9 | 4.1 | n.d. (4.1) |
| Ala[3] | 6.5 | 6.5 | n.d. (6.7) | 6.6 |
| Ala[4] | n.d. | 6.0 | 5.9 | n.d. (6.2) |
| Gln[7] | 4.2 | n.d. | 4.8 | 5.0 |
| Ile[9] | 5.1 | 5.9 | n.d. (6.1) | n.d. (6.0) |
| Gly[11] | 4.4 | 4.9 | 5.0 | 5.0 |
| Leu[12] | 7.3 | 7.7 | 7.7 | 7.7 |
| Val[15] | n.d. | 7.7 | 7.7 | 7.8 |
| Gln[18] | 5.1 | 5.4 | n.d. (5.4) | n.d. (5.6) |
| Gln[19] | n.d. | n.d. | 7.7 | 7.9 |
| Pheol[20] | 9.2 | 9.2 | 9.1 | n.d. |

[a] The values at 20 °C are shown in parentheses. [b] The figures in parentheses represent the values at 35 °C. n.d., Not determined.

**Table 2** Comparison of $^3J_{NH-C_\alpha H}$-values of trichosporin B-V[a] and des-Pro[14]-trichosporin B-V in $CD_3OH$ at 27 °C (5 mmol $dm^{-3}$)

| Residue | TS-B-V $J$/Hz | des-Pro[14]-TS-B-V $J$/Hz |
|---|---|---|
| Ala[2] | 4.1 | n.d. |
| Ala[3] | n.d. | 6.6 |
| Ala[4] | 6.0 | 5.9 |
| Gln[7] | 4.7 | 4.7 |
| Ile[9] | 6.1 | 5.6 |
| Gly[11] | 5.0 | 4.0 |
| Leu[12] | 7.8 | 4.7 |
| Val[15] | 7.8 | 5.9 |
| Gln[18] | n.d. | 5.8 |
| Gln[19] | n.d. (7.5) | 7.5 |
| Pheol[20] | n.d. (9.2) | 9.1 |

[a] The values at 10 mmol $dm^{-3}$ are shown in parentheses. n.d., Not determined.

**Table 3** Hydrogen–deuterium (H–D) exchange rates of the amide protons at 27 °C

| | Time ($t$/h)[a] | | |
|---|---|---|---|
| Aib[1] | ≪0.25 | Gly[11] | ~15 |
| Ala[2] | ≪0.25 | Leu[12] | >24 |
| Ala[3] | ~2 | Aib[13] | ~12 |
| Ala[4] | ~3 | Pro[14] | |
| Aib[5] | ~3 | Val[15] | ≫24 |
| Aib[6] | ≫24 | Aib[16] | >24 |
| Gln[7] | ≫24 | Aib[17] | ≫24 |
| Aib[8] | ≫24 | Gln[18] | ≫24 |
| Ile[9] | ≫24 | Gln[19] | >24 |
| Aib[10] | ≫24 | Pheol[20] | >24 |

[a] Exchange rates are expressed as the time taken for the peak height to decrease to 50% of its initial value.

40 °C. On the other hand, most values became slightly smaller at −5 °C. We suggest that the helical structure becomes a little tighter at this temperature.

*Determination of Hydrogen-bonded Amide Protons.*—In order to examine amide protons involved in intramolecular hydrogen bonding, hydrogen–deuterium (H–D) exchange rates[12,13] of the NH protons were obtained at 27 °C by replacing $CD_3OH$ with $CD_3OD$ (Fig. 2). The exchange rates obtained here (Table 3) can be divided into the following three groups.

(i) *N-Terminal dipeptide, Aib[1] and Ala[2].* The NH signals for Aib[1] and Ala[2] disappeared within 15 min of change of solvent of $CD_3OD$ for $CD_3OH$, as did the carboxamide protons of three Gln residues. This observation indicates that these protons are not involved in intramolecular hydrogen bonding and are always exposed to the solvent.

(ii) *Ala[3], Ala[4] and Aib[5].* These NH protons showed rapid exchange rates. However, they exchanged more slowly than did the Aib[1] and Ala[2] NH protons. This observation suggests that the conformational constraints of these protons are different from those of Aib[1] and Ala[2]. Considering that these protons in proximity to the *N*-terminus are apt to be greatly influenced by the solvent, they are expected to participate in hydrogen bonding to some extent. Participation of the Ala[3] NH proton in hydrogen bonding suggests that at least one 4 ⟶ 1 hydrogen bond exists between the acetyl CO oxygen and this NH proton.

(iii) *Segment* 6–20. The very slow exchange rates of these NH protons are indicative that they are strongly hydrogen bonded. Among these exchange rates, those of Gly[11] and Leu[12] were relatively rapid. This does not signify that the Gly[11] and Leu[12] NH protons participate in weaker hydrogen bonding, because the structure is very rigid according to the small temperature

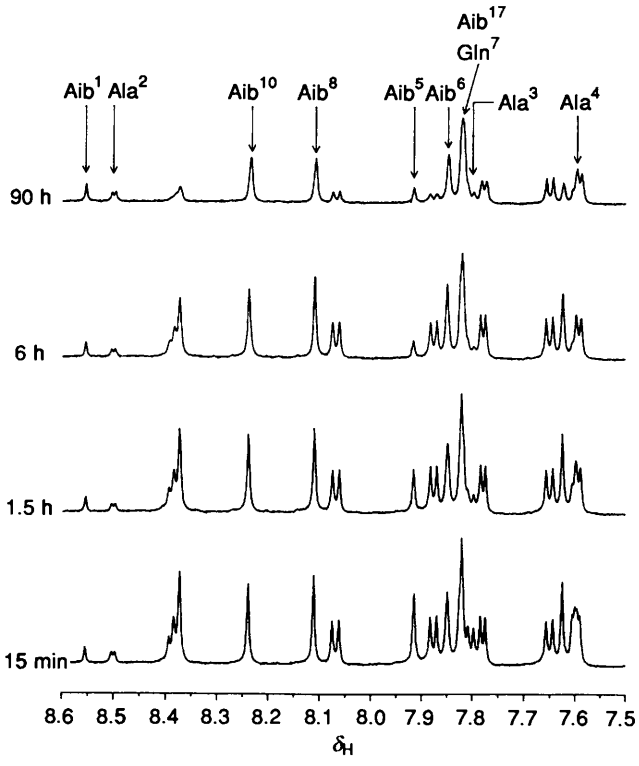


**Fig. 2** Spectral changes in the amide proton region of trichosporin B-V in $CD_3OD$ (27 °C; ~7 mmol $dm^{-3}$). The sample was kept at 27 °C for the first 24 h and, after that, at 23 °C except during the measurements.

dependence of the $^3J_{NH-C_\alpha H}$-values. Therefore we deduce that these rapid exchange rates reflect the large extent of solvent exposure of these hydrogens.

*Determination of Secondary Structure.*—From the evidence obtained so far, TS-B-V is thought to be entirely elongated in a rigid helical structure. More detailed information on the structure of this peptide was obtained through the observation of phase-sensitive nuclear Overhauser enhancement (NOESY) spectra (Figs. 3, 4 and 5). Table 4 summarizes inter-residual NOE data.[14]

As described already,[5] successive short-distance NOEs [$d_{NN}(i, i + 1)$-type] were discerned from Aib[1] to Aib[13]. In addition to this regularity, other diagnostic NOEs [$d_{NN}(i, i + 2)$-, $d_{\alpha N}(i, i + 1)$-, $d_{\alpha N}(i, i + 3)$-, $d_{\alpha\beta}(i, i + 3)$- and $d_{\beta N}(i, i + 1)$-type] strongly suggested the formation of a regular helical structure between Ac-Aib and Aib[13]; it is an α-helix or a $3_{10}$-helix. Additional characteristic NOEs [$d_{\alpha N}(i, i + 4)$-type; $i = 4$ and 9] are indicative of the prevalence of an α-helical structure at least between Ala[4] and Aib[13] which is stabilized by 5 ⟶ 1 hydrogen bonds ($CO_i$-$NH_{i+4}$). Thus, the NH protons from Aib[8] to Aib[13] would participate in the hydrogen bonding. Furthermore, the Aib[6] and Gln[7] NH protons, showing very slow H–D exchange rates, also would be hydrogen bonded to the Ala[2] and Ala[3] CO oxygens in a 5 ⟶ 1 fashion, in order to stabilize the α-helix. The most probable hydrogen bonding pattern in this region is schematically illustrated in Fig. 6(a).

Regular helical conformations in polypeptide chains are often broken by a Pro residue. In the case of TS-B-V, the connectivities from the Aib[13] NH proton to the Pro[14] $C^\delta H_2$ protons and from the Pro[14] $C^\delta H_2$ protons to the Val[15] NH proton were discerned, which are considered equivalent to the NH–NH connectivities[15] from Aib[13] to Val[15]. In addition to this observation, additional specific NOEs [$d_{NN}(i, i + 2)$-type, $i = 13$; $d_{\alpha N}(i, i + 3)$-type, $i = 12$; and $d_{\alpha\beta}$ $(i, i + 3)$-type, $i = 12$] strongly suggest the possibility that the Pro residue is

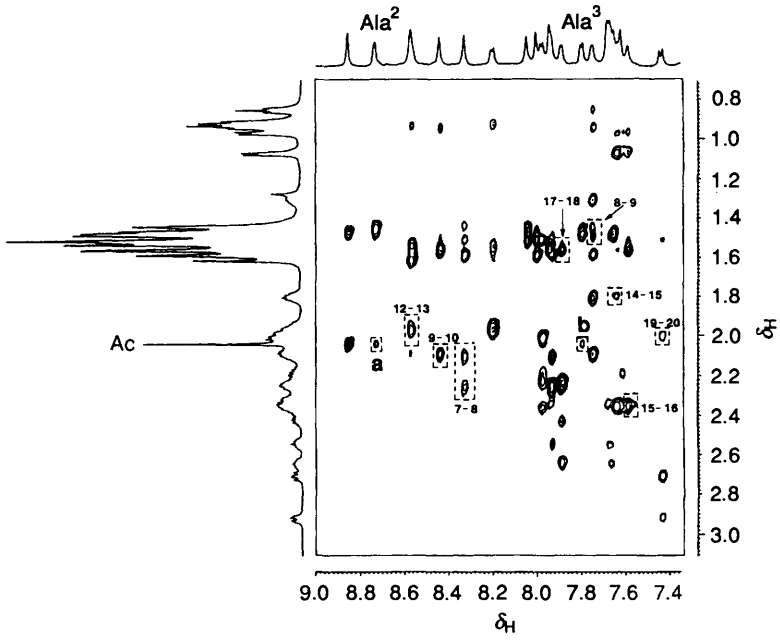


**Fig. 3** NH-aliphatic region of the NOESY spectrum of trichosporin B-V in $CD_3OH$ (−5 °C; 30 mmol $dm^{-3}$). Eight $d_{\beta N}(i, i + 1)$-type cross-peaks were identified. The acetyl $C^{\beta}H_3$ protons indicated connectivities with the $Ala^2$ and $Ala^3$ NH protons (cross-peaks **a** and **b**). These cross-peaks were very weak at 10 °C.

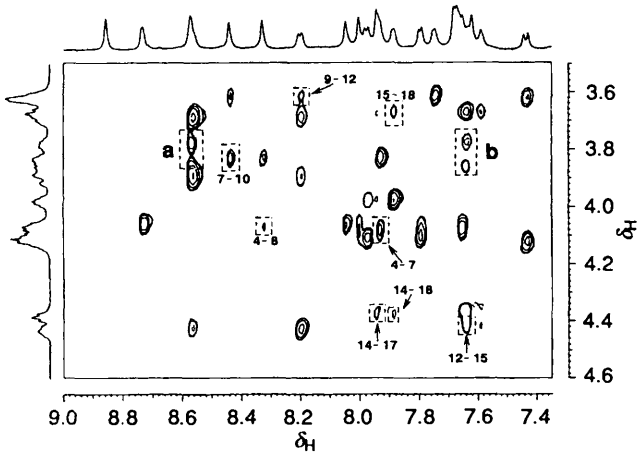


**Fig. 4** Fingerprint region of the NOESY spectrum of trichosporin B-V in $CD_3OH$ (−5 °C; 30 mmol $dm^{-3}$). NOE cross-peaks [$d_{\alpha N}(i, i + 3$ or $i + 4)$-type] are shown. Some cross-peaks disappear at this counter level. The cross-peaks **a** and **b** stand for connectivities of the $Pro^{14}$ $C^{\delta}H_2$ protons with the $Aib^{13}$ and $Val^{15}$ NH protons, respectively.

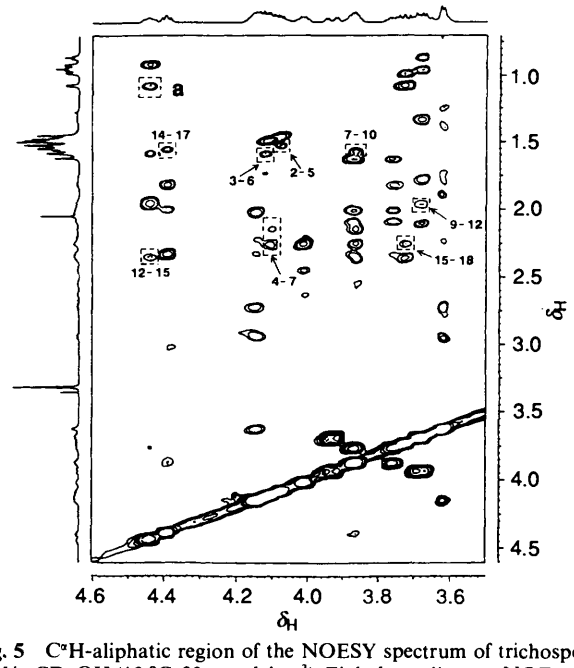


**Fig. 5** $C^{\alpha}H$-aliphatic region of the NOESY spectrum of trichosporin B-V in $CD_3OH$ (10 °C; 30 mmol $dm^{-3}$). Eight long-distance NOE cross-peaks [$d_{\alpha\beta}$ $(i, i + 3)$-type] were identified.

involved in the *N*-terminal α-helix. However, if the Pro residue were arranged as a constituent of the α-helix which is stabilized by 5 ⟶ 1 hydrogen bonding [Fig. 6(b)], the side-chain ring would cause serious steric repulsions for the $Aib^{10}$ CO oxygen and the $Aib^{13}$ $C^{\beta}H_3$ group judging from inspection of molecular models. It is thus presumed that, in order for the above three groups to be free from steric repulsions, the $Leu^{12}$ CO oxygen is hydrogen bonded to the $Val^{15}$ NH proton (4 ⟶ 1 type, $CO_i$–$NH_{i+3}$) rather than to the $Aib^{16}$ NH proton (5 ⟶ 1 type) as shown in Fig. 6(c). Therefore, the helix is considered to be twisted around the $Pro^{14}$ residue. The NOE cross-peak between the $Leu^{12}$ $C^{\alpha}H$ proton and $Val^{15}$ $C^{\gamma}H_3$ protons supports this structure (Fig. 5); inspection of molecular models shows that these protons are near to each other. This interposition of 4 ⟶ 1 type hydrogen bonding would make it reasonable for $Leu^{12}$ and $Val^{15}$ to have a slightly larger than normal $^3J_{NH-C\alpha H}$ values and leads to the result that the $Aib^{10}$ and $Gly^{11}$ CO oxygens do not participate in hydrogen bonding.

Although completely subsequent NH–NH connectivities were not observed between $Pro^{14}$ and $Pheol^{20}$, structural regularity can evidently be recognized in this region through the observation of typical NOE patterns characteristic of an α-helical structure. Some diagnostic NOE cross-peaks [$d_{\alpha N}$ $(i, i + 4)$-type, $i$ = 14 and 15; and $d_{\alpha\beta}$ $(i, i + 3)$-type, $i$ = 14 and 15] and the finding that the $Gln^{18}$, $Gln^{19}$ and $Pheol^{20}$ NH protons participate in hydrogen bonding shows the prevalence of an α-helical structure between $Pro^{14}$ and $Pheol^{20}$, which is stabilized by the 5 ⟶ 1 hydrogen bonds as shown in Fig. 6(a). Taking account of the α-helicity, the $Aib^{17}$ NH proton, which showed extremely slow H–D exchange rates, are thought to be hydrogen bonded to the $Aib^{13}$ CO oxygen in 5 ⟶ 1 fashion. Thus, the $Aib^{16}$ NH proton is unlikely to participate in hydrogen bonding [Fig. 6(d)]. In this case, the slow H–D exchange of the NH

**Table 4** Inter-residual NOEs observed in $CD_3OH$ at −5 and 10 °C (30 mmol $dm^{-3}$)

| Residue | 0[a] | 1 | 2 | 3 | 4 | 5 | 6 | 7 | 8 | 9 | 10 | 11 | 12 | 13 | 14[b] | 15 | 16 | 17 | 18 | 19 | 20 |
|---|---|---|---|---|---|---|---|---|---|---|---|---|---|---|---|---|---|---|---|---|---|
| $d_{NN}(i, i+1)$ | | ○ | ○ | ○ | ○ | ○ | ○ | ○ | ○ | ○ | ○ | ○ | ○ | ○ | [○] | | ○ | | ○ | ○ | |
| $d_{NN}(i, i+2)$ | | | | ● | ● | | ● | | ● | | | | | ● | | | | | ● | | |
| $d_{\alpha N}(i, i+1)$ | △ | | | | △ | | | △ | | △ | | △ | △ | | △ | | | | △ | | |
| $d_{\alpha N}(i, i+2)$ | ▲ | | | | | | | | | | | | | | | | | | | | |
| $d_{\alpha N}(i, i+3)$ | ◇ | | | ◇ | ◇ | | | ◇ | | ◇ | | | ◇ | | ◇ | ◇ | | | | | |
| $d_{\alpha N}(i, i+4)$ | | | | | ◆ | | | | | ◆ | | | | | ◆ | ◆ | | | | | |
| $d_{\alpha\beta}(i, i+3)$ | | | ☆ | ☆ | ☆ | | | ☆ | | ☆ | | | ☆ | | ☆ | ☆ | | | | | |
| $d_{\beta N}(i, i+1)$ | | | | | | | | ★ | ★ | ★ | | | ★ | | ★ | ★ | | ★ | | ★ | |

[a] Residue 0 stands for an acetyl group. [b] The Pro $C^{\delta}H_2$ protons are regarded as NH protons.

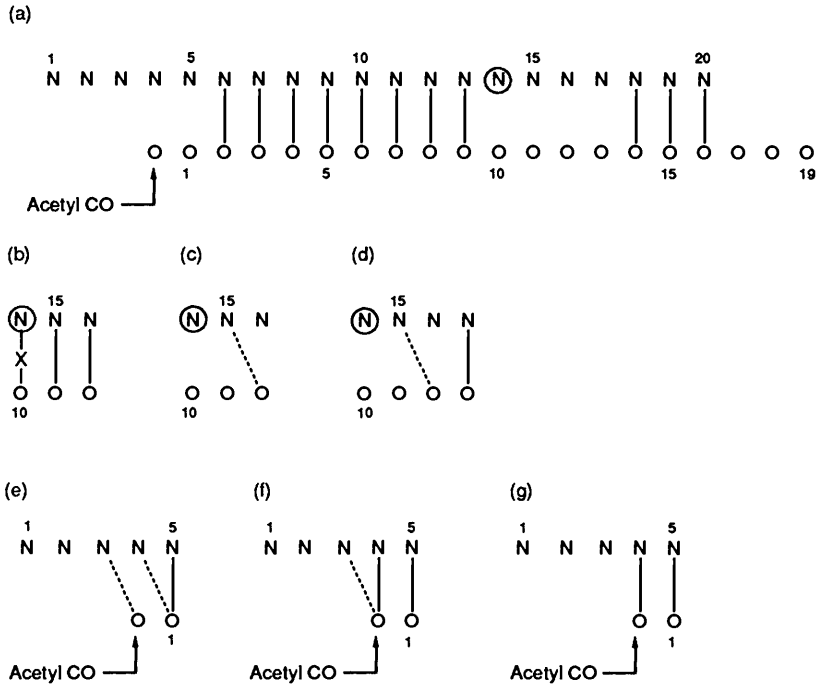


**Fig. 6** Intramolecular hydrogen bonding patterns of trichosporin-B-V. Solid and broken lines stand for 5 ⟶ 1 and 4 ⟶ 1 hydrogen bonding, respectively.

proton can be interpreted by the inaccessibility of the solvent which arises from conformational constraints.[16]

The remaining problem is the determination of the first turn. The presence of a 4 ⟶ 1 hydrogen bond (acetyl CO ⟶ $Ala^3$ NH, $CO_i$–$NH_{i+3}$) suggested in the H–D exchange experiment increases the possibility that the first turn is a $3_{10}$-helix as proposed in trichorzianines[17] whose *N*-terminal sequences are Ac-Aib-Ala-Ala-Aib-Aib or -Iva (Iva = isovaline). This possibility is supported by an NOE cross-peak characteristic of a $3_{10}$-helix [$d_{\alpha N}$ ($i$, $i$ + 2)-type] which was observed between the acetyl $CH_3$ protons and the $Ala^2$ NH proton at −5 °C (Fig. 3). In this case, the $Ala^4$ and $Aib^5$ NH protons are presumed to be hydrogen bonded predominantly to the $Aib^1$ CO oxygen. This hydrogen bonding pattern is more likely than that of Fig. 6(f), judging from the almost identical H–D exchange rates of $Ala^4$ and $Aib^5$ and the spatial proximity between the acetyl $CH_3$ protons and the $Ala^2$ NH proton. On the other hand, such hydrogen bonding patterns as shown in Fig. 6(g) could be ruled out completely at −5 °C by the lack of a diagnostic NOE [$d_{\alpha N}$ ($i$, $i$ + 4)-type, $i$ = 0]. Therefore, the first three amino acid residues are most likely to be arranged in a $3_{10}$-helical fashion. Few characteristic NOE cross-peaks which define the secondary structure clearly were obtained from the NOESY spectra recorded at 27 °C. Considering the strong intramolecular hydrogen bonding and temperature-independent $^3J_{NH-C\alpha H}$-values, it is expected that the structure at 27 °C is almost the same as that at −5 °C. In conclusion, the secondary structure of TS-B-V obtained here is very close to that of alamethicin reported by Campbell and co-workers,[16] except for the first turn. We have already noticed that the secondary structures of TS-Bs are very similar to each other and that the lipophilicity of TS-Bs affect catecholaminic secretion[18,19] from bovine adrenal chromaffin cells.[5] In the course of this study, furthermore, we found that des-$Pro^{14}$-TS-B-V does not show the activity.[20] This finding suggests that the twisted structure of TS-Bs is a key structure causing the interaction between the peptide molecules and cell membranes.

## Experimental

The CD spectra were recorded on a JASCO J-720 spectropolarimeter.

For NMR experiments, the dried and purified samples were dissolved in $CD_3OH$ or $CD_3OD$ (0.35 $cm^3$) containing $SiMe_4$ as internal standard. All NMR spectra were recorded on a Bruker AM-600 (600 MHz) spectrometer. The details of NMR measurements have already been described in the preceding paper.[5]

## Acknowledgements

This work was supported in part by a Grant-in-Aid for

Scientific Research from the Ministry of Education, Science and Culture of Japan (01771913 and 63303013) and by the Foundation for the Promotion on Medicinal Resources. We thank Dr. M. R. Wälchli (Bruker Japan Co., Ltd.) for important advice on the measurement of NMR spectra.

## References

1 T. Fujita, A. Iida, S. Uesato, Y. Takaishi, T. Shingu, M. Saito and M. Morita, *J. Antibiot.*, 1988, **41**, 814.
2 A. Iida, M. Okuda, S. Uesato, Y. Takaishi, T. Shingu, M. Morita and T. Fujita, *J. Chem. Soc., Perkin Trans. 1*, 1990, 3249.
3 R. C. Pandy, J. C. Cook, Jr. and K. L. Rinehart, Jr., *J. Am. Chem. Soc.*, 1977, **99**, 8469.
4 E. Katz, M. Aydin, N. Lucht, W. A. König, T. Ooka and G. Jung, *Liebigs Ann. Chem.*, 1985, 1041.
5 A. Iida, S. Uesato, T. Shingu, M. Okuda, Y. Nagaoka, Y. Kuroda and T. Fujita, preceding paper.
6 G. Jung, N. Dubischar and D. Leibfritz, *Eur. J. Biochem.*, 1975, **54**, 395.
7 G. Irmscher, G. Bovermann, G. Boheim and G. Jung, *Biochim. Biophys. Acta*, 1978, **507**, 470.
8 H. Schmitt, W. Winter, R. Bosch and G. Jung, *Liebigs Ann. Chem.*, 1982, 1304.
9 A. Pardi, M. Billeter and K. Wüthrich, *J. Mol. Biol.*, 1984, **180**, 741.
10 U. Banerjee, F. P. Tsui, T. N. Balasubramanian, G. R. Marshall and S. I. Chan, *J. Mol. Biol.*, 1983, **165**, 757.
11 A. Iida, S. Yoshimatsu, M. Sanekata and T. Fujita, *Chem. Pharm. Bull.*, 1990, **38**, 2997.
12 D. G. Davis and B. F. Gisin, *FEBS Lett.*, 1981, **133**, 247.
13 P. Štrop and K. Wüthrich, *J. Mol. Biol.*, 1983, **166**, 631.
14 K. Wüthrich, M. Billeter and W. Braun, *J. Mol. Biol.*, 1984, **180**, 715.
15 R. Bazzo, M. J. Tappin, A. Pastore, T. S. Harvey, J. A. Carver and I. D. Campbell, *Eur. J. Biochem.*, 1988, **173**, 139.
16 G. Eposito, J. A. Carver, J. Boyd and I. D. Campbell, *Biochemistry*, 1987, **26**, 1043.
17 B. Bodo, S. Rebuffat, M. E. Hajii and D. Davoust, *J. Am. Chem. Soc.*, 1985, **107**, 6011.
18 E. Tachikawa, T. Kashimoto, A. Iida, Y. Nagaoka, T. Fujita and Y. Takaishi, *J. Pharmacobio-Dyn.*, 1991, **14**, S-106.
19 E. Tachikawa, S. Takahashi, K. Furumachi, T. Kashimoto, A. Iida, Y. Nagaoka, T. Fujita and Y. Takaishi, *Mol. Pharmacol.*, 1991, **40**, 790.
20 E. Tachikawa, T. Kashimoto, A. Iida, Y. Nagaoka, T. Fujita and Y. Takaishi, unpublished work.

*Paper* 2/04596F
*Received* 26*th August* 1992
*Accepted* 24*th September* 1992